Polymer 49 (2008) 3029–3041

Contents lists available at ScienceDirect

Polymer

journal homepage: www.elsevier.com/locate/polymer

The influence of crosslinking and fumed silica nanoparticles on mixed gas transport properties of poly[1-(trimethylsilyl)-1-propyne]

Scott D. Kelman [a], Roy D. Raharjo [a], Christopher W. Bielawski [b], Benny D. Freeman [a,*]

[a] Center for Energy and Environmental Resources, Department of Chemical Engineering, The University of Texas at Austin, 10100 Burnet Road, Building 133, Austin, TX 78758, United States
[b] Department of Chemistry and Biochemistry, The University of Texas at Austin, Austin, TX 78712, United States

ARTICLE INFO

Article history:
Received 4 February 2008
Received in revised form 26 March 2008
Accepted 29 March 2008
Available online 11 April 2008

Keywords:
PTMSP
Crosslinking
Permeability

ABSTRACT

Crosslinking poly[1-(trimethylsilyl)-1-propyne] (PTMSP) films with 3,3′-diazidodiphenylsulfone, a bis(azide) crosslinker, rendered the films insoluble in common solvents for PTMSP such as toluene. At all temperatures, mixed gas CH_4 and n-C_4H_{10} permeabilities of crosslinked PTMSP were less than those of uncrosslinked PTMSP, which correlates with lower free volume in the crosslinked material. The presence of fumed silica (FS) nanoparticles in both uncrosslinked PTMSP and crosslinked PTMSP increased mixed gas CH_4 and n-C_4H_{10} permeabilities, consistent with the disruption of polymer chain packing by such nanoparticles. Mixed gas CH_4 permeabilities of all films were significantly less than their corresponding pure gas CH_4 permeabilities. For example, at 35 °C, the mixed gas CH_4 permeabilities were approximately 60–80% less than their pure gas values. The greatest decrease was observed for uncrosslinked PTMSP, while nanocomposite PTMSP films showed the least decrease. The mixed gas n-C_4H_{10}/CH_4 selectivities of crosslinked PTMSP and nanocomposite PTMSP films were less than those of uncrosslinked PTMSP at all temperatures. For example, at 35 °C, the mixed gas n-C_4H_{10}/CH_4 selectivities of uncrosslinked PTMSP, crosslinked PTMSP containing 10 wt% crosslinker, and uncrosslinked PTMSP containing 30 wt% FS were 33, 27, and 17, respectively, when the feed gas contained 2 mol% n-C_4H_{10} and the total upstream mixture fugacity was 11 atm. For all films, as temperature decreased, mixed gas n-C_4H_{10} permeabilities increased, and mixed gas CH_4 permeabilities decreased. Consequently, the mixed gas n-C_4H_{10}/CH_4 selectivities increased substantially as temperature decreased and the mixed gas selectivity of uncrosslinked PTMSP increased from 33 to 170 as temperature decreased from 35 °C to −20 °C when the feed gas contained 2 mol% n-C_4H_{10} and the total upstream mixture fugacity was 11 atm.

Published by Elsevier Ltd.

1. Introduction

The removal of higher hydrocarbons from natural gas is an important separation that has been identified as a growth area for polymer membranes [1]. An ideal membrane for this separation would be more permeable to higher hydrocarbons (*i.e.*, C_{3+} compounds) than to CH_4 [2]. In this case, the CH_4 rich product would be retained at or near feed pressure, thus minimizing the need for repressurization following the membrane separation. Membrane materials exhibiting such characteristics are often referred to as "reverse selective" materials since they are more permeable to larger, but more soluble, molecules than to smaller, less soluble, molecules, which is opposite to the trend often observed in glassy polymers [1–5]. Poly[1-(trimethylsilyl)-1-propyne] (PTMSP) is a reverse selective polymer having high vapor/gas selectivity [6–9]. For example, the n-C_4H_{10}/CH_4 mixed gas selectivity is 35 at 25 °C [10]. Additionally, PTMSP is the most permeable polymer known [11,12], and the high permeability is attributed, in part, to its very high fractional free volume (FFV) [13] of 0.29 [14]. The exceptionally high FFV contributes to PTMSP being weakly size-sieving, which, in turn, assists it in being more permeable to large gas or vapor molecules than to smaller molecules [13].

The free volume elements of PTMSP are thought to be interconnected [8,13], and the majority of the gas permeation is believed to occur through these interconnected free volume elements [8,15]. The transport mechanism of condensable vapors such as n-C_4H_{10} in PTMSP has been suggested to be similar in some regards to condensable vapor transport in microporous and nanoporous carbon membranes and Vycor glass membranes [16–21]. In such materials, the condensable vapor sorbs onto the walls of the small pores, and diffuses along the pore walls. Multilayer absorption of condensable components, which can partially or completely block the pores, reduces the flow of less condensable gases. In this regard,

* Corresponding author. Tel.: +1 512 232 2803; fax: +1 512 232 2807.
E-mail address: freeman@che.utexas.edu (B.D. Freeman).

0032-3861/$ – see front matter Published by Elsevier Ltd.
doi:10.1016/j.polymer.2008.03.053

CH_4 permeability in PTMSP at 23 °C decreased from 15,400 barrer in pure methane to 1800 barrer when a mixture of 98 mol% CH_4 and 2 mol% n-C_4H_{10} was permeated across the film [8]. Raharjo et al. studied the transport of n-C_4H_{10}/CH_4 mixtures in PTMSP, and the decrease in mixed gas CH_4 permeability was caused by a decrease in both mixed gas CH_4 solubility and diffusivity in the presence of n-C_4H_{10} [22]. Competitive sorption effects caused a decrease in CH_4 solubility, and filling the free volume elements with sorbed n-C_4H_{10} also caused CH_4 diffusivity to decrease. At all temperatures and pressures considered, the relative decrease in CH_4 solubility was slightly greater than the relative decrease in CH_4 diffusivity [22].

The solvent resistance of PTMSP is low, and it is soluble in a wide range of organic solvents [23]. This high solubility can compromise the utility of PTMSP in natural gas separations, when aliphatic and aromatic contaminants may be present in the feed stream [10]. The pure gas permeability of PTMSP to gases and vapors decreases over time due to physical aging, which is the gradual relaxation of nonequilibrium excess free volume [7,15,24–29]. However, in a vapor/gas environment, physical aging is substantially reduced [7] because condensable gases such as n-C_4H_{10} are thought to fill the nonequilibrium excess free volume of the polymer, thereby stabilizing free volume elements that are susceptible to aging. To improve the performance of PTMSP in vapor/gas separations, it would be useful to increase its solvent resistance and control physical aging.

Crosslinking PTMSP with bis(azide)s increases its solvent resistance remarkably, and crosslinked films are insoluble in common PTMSP solvents such as toluene, cyclohexane, and tetrahydrofuran [30–33], all of which are good solvents for uncrosslinked PTMSP [12,23]. The addition of fumed silica (FS) nanoparticles did not alter the solubility characteristics. That is, uncrosslinked nanocomposite PTMSP films were soluble in toluene, while crosslinked nanocomposite films were not [33]. The crosslinking reaction harnesses the ability of an azide (R-N_3) to decompose at elevated temperatures to form a reactive nitrene and molecular nitrogen (N_2) [31]. The resulting nitrene can abstract hydrogen from the allyl side group of PTMSP [31]. The hydrogen abstraction is believed to be from the allyl side group rather than from the trimethylsilyl side group, because the C–H bond energy in the allyl side group ($\sim$85 kcal/mol) [34] is significantly less than that of the C–H bonds in the $Si(CH_3)_3$ ($\sim$100 kcal/mol) side group [34,35]. Furthermore, cycloaddition reactions between the incipient nitrenes and the double bonds of the PTMSP backbone (to form the respective aziridines) are believed to be minimal because the FT-IR signals characteristic of the alkenes in PTMSP (1600 cm^{-1}, C=C stretching) did not decrease in intensity upon crosslinking [33]. Finally, the azide decomposition process yields nitrogen gas and reactive nitrenes as the exclusive products, so virtually no side-products are formed that might contaminate the polymer [31].

Crosslinking decreases both pure and mixed gas permeabilities of PTMSP [30–33], and the decrease is correlated with a decrease in free volume upon crosslinking [33]. Furthermore, at 35 °C, the mixed gas n-C_4H_{10}/CH_4 selectivity of crosslinked PTMSP was slightly less than that of uncrosslinked PTMSP. The lower free volume and increased size-sieving behavior in crosslinked PTMSP is consistent with lower permeability and lower n-C_4H_{10}/CH_4 mixture selectivity in the crosslinked films [33]. The addition of FS nanoparticles to PTMSP increases pure and mixed gas permeabilities [10,33,36,37]. However, mixed gas n-C_4H_{10}/CH_4 selectivity of nanocomposite PTMSP is lower than that of uncrosslinked PTMSP [10,33], so the extra free volume created by FS addition may be sufficient to permit access to transport processes, such as Knudsen flow, which favor CH_4 permeation over that of n-C_4H_{10} [10].

In this study, mixed gas transport properties of PTMSP were investigated using a 98 mol% CH_4 and 2 mol% n-C_4H_{10} gas mixture. This composition was chosen because it is used in the literature to model higher hydrocarbon removal from natural gas [8,10,22,33,38]. The effects of crosslinking and addition of FS nanoparticles to PTMSP on the mixed gas transport properties are reported. The mixed gas transport properties are reported at 35 °C, 10 °C, 0 °C, and −20 °C. These temperatures were chosen to provide a more complete fundamental understanding of the impact of nanoparticle addition and crosslinking on the gas separation properties and because natural gas separations are performed over this temperature range [1]. The feed gas pressure was varied to understand its influence on mixed gas transport properties. Permeability hysteresis or conditioning effects were investigated in this study by measuring mixed gas permeabilities when the films were depressurized from their maximum pressure. Conditioning was identified if an increase in permeability occurred during depressurization [39]. These effects have been studied for pure gas permeation in PTMSP [40–42], but conditioning of PTMSP by vapor/gas mixtures has not been extensively investigated.

2. Theory

The permeability of a polymer film to gas A, P_A, is defined as follows [43,44]:

$$P_A = \frac{N_A l}{f_{2A} - f_{1A}} \tag{1}$$

where N_A is the steady state gas flux through the film (cm^3(STP)/(cm^2 s)), l is the film thickness (cm), and f_{2A} and f_{1A} are the upstream and downstream fugacities of A (cmHg). Permeability coefficients are often expressed in units of barrer, where 1 barrer = 1×10^{-10} cm^3(STP)cm/(cm^2 s cmHg).

Fugacity is often replaced by partial pressure in Eq. (1) if the gas is ideal [45]. Significant non-ideality can be displayed by n-C_4H_{10}/CH_4 gas mixtures [45], so fugacity is used for all gas transport calculations in this study. The fugacity of gas A is calculated as follows [46]:

$$f_A = \phi_A x_A p \tag{2}$$

where ϕ_A is the fugacity coefficient of A, x_A is the mole fraction of A, and p is the total pressure (atm). The detailed procedure used to calculate the fugacity coefficients is provided elsewhere [47].

The solution-diffusion model is often used to describe the transport of gas molecules in dense polymeric membranes [48]. The gas transport is thought to occur via a three-step mechanism wherein gas dissolves on the feed (high pressure) side of the film, then diffuses across the film, and desorbs from the permeate (low pressure) side of the film. If the diffusion process is Fickian, the permeability coefficient is given by [44]:

$$P_A = \frac{C_{2A} - C_{1A}}{f_{2A} - f_{1A}} \times D_A \tag{3}$$

where C_{2A} and C_{1A} are the upstream and downstream concentrations of A in the polymer (cm^3(STP)/cm^3 polymer), and D_A is the concentration-averaged effective diffusion coefficient (cm^2/s). If the permeate pressure is significantly less than the feed pressure, so that $C_{2A} \gg C_{1A}$ and $f_{2A} \gg f_{1A}$, then the permeability of gas A can be expressed as [3]:

$$P_A = D_A S_A \tag{4}$$

where S_A is the apparent solubility coefficient of gas A in the polymer (cm^3(STP)/(cm^3 polymer cmHg)), which is C_{2A}/f_{2A}.

The ideal selectivity of a membrane for gas A over gas B is the ratio of gas permeability coefficients. Generally the most permeable gas is in the numerator of the following expression [3]:

$$\alpha_{A/B} = \frac{P_A}{P_B} = \left[\frac{D_A}{D_B}\right]\left[\frac{S_A}{S_B}\right] \quad (5)$$

where D_A/D_B is the diffusivity selectivity, which is the ratio of the diffusion coefficients of gases A and B. Generally, smaller gas molecules have larger diffusion coefficients than larger gas molecules [44]. The solubility selectivity, S_A/S_B, is the ratio of the solubility coefficients of gases A and B. The mixed gas permeability selectivities in this study are expressed as the ratio of mixed gas permeabilities, which are calculated using the mixed gas fugacities. If permeabilities are calculated in terms of fugacities, rather than partial pressures, then the ideal selectivity in Eq. (5) does not reduce to the ratio of mole fractions of components A and B in the product streams (*i.e.*, the separation factor), and it will do so if the permeabilities are defined based upon partial pressure driving forces [44,49]. However, since the focus of this work is on materials science of transport in polymers, it is useful to separate effects due to non-ideal gas behavior from the fundamental transport properties of the material, so we adopt the definition of permeability in Eq. (1).

The influence of temperatures on gas permeability is typically described as follows [3]:

$$P = P_0 \exp\left[\frac{-E_P}{RT}\right] \quad (6)$$

where P_0 is a preexponential factor, and E_P is the activation energy of permeation. This model was developed for polymers in which the transport properties do not change markedly with pressure. If the permeability properties change significantly with pressure (or fugacity), then this framework must be applied with caution to the experimental data [50].

3. Experimental

3.1. Materials

Cylinders of chemical purity (99%) CH_4 and n-C_4H_{10} were received from Air Gas Southwest Inc. (Corpus Christi, TX) and were used in the pure gas permeation measurements. Mixtures of CH_4 and n-C_4H_{10} were received from Air Liquide America Corporation (Houston, TX). All gases were used as-received. Poly[1-(trimethylsilyl)-1-propyne] (PTMSP) was kindly supplied by Air Products and Chemicals, Inc. PTMSP was crosslinked using 3,3′-diazidodiphenylsulfone, a bis(azide) crosslinker, which was supplied by Sigma–Aldrich Chemicals. This bis(azide) is safe at the conditions of film formation and crosslinking, and it crosslinks polymeric materials effectively [33,51]. Nonporous, hydrophobic fumed silica nanoparticles, with a characteristic dimension of 13 nm (Cab-O-Sil TS-530, from Cabot Corp., Tuscola, IL), were added to PTMSP to form nanocomposite films. In their manufacturing process, TS-530 FS nanoparticles are chemically treated with hexamethyldisilazane, which replaces the hydrophilic hydroxyl surface groups with hydrophobic trimethylsilyl surface groups [52]. All solvents used in the experiments had a purity of at least 99.8%.

3.2. Film preparation

Dense films of PTMSP and bis(azide) crosslinker (XL) were cast on glass plates from a toluene solution containing 1.5 wt% polymer. The solutions were stirred for 2 days using a magnetic stir bar. Nanocomposite PTMSP films were formed by adding FS nanoparticles to these solutions. The solution cast films were dried at ambient conditions for approximately 1 week until all toluene had evaporated. The reported wt% of crosslinker or FS in a film, w_A, is given by:

$$w_A = \frac{m_A}{m_A + m_p} \quad (7)$$

where m_A is the crosslinker or FS mass, and m_p is the polymer mass. This calculation is based on the films before they are crosslinked. The dried films were then removed from the glass plates before being thermally annealed in a vacuum oven at 180 °C for 90 min to crosslink them. Films without crosslinker were subjected to the same heat treatment as films containing bis(azide) crosslinker, which insures that all films had as similar a thermal history as possible. The crosslinking reaction was performed in the absence of oxygen to prevent the newly formed nitrenes from oxidizing to their respective nitroso derivatives, which ultimately leads to reduced crosslinking efficiencies [53]. A temperature of 180 °C was required to facilitate the formation of a bis(nitrene) from the bis(azide) crosslinker. At lower temperatures, the crosslinking reaction did not progress at a reasonable rate. Furthermore, the aryl azide signal at 2120 cm^{-1} in the FT-IR spectra of these films disappeared after 90 min in the vacuum oven, indicating that the bis(azide) crosslinker quantitatively reacted under these conditions [33].

The transport properties, FFV, and positron annihilation lifetime spectroscopy parameters of PTMSP display strong hysteresis effects [26,27,29,54,55]. Consequently, it is important to prepare each film in as similar a fashion as possible. During film preparation and crosslinking, exposure of the films to contaminants such as vacuum pump oil vapor is minimized, because these materials alter the transport properties of PTMSP [55]. The contamination by vacuum

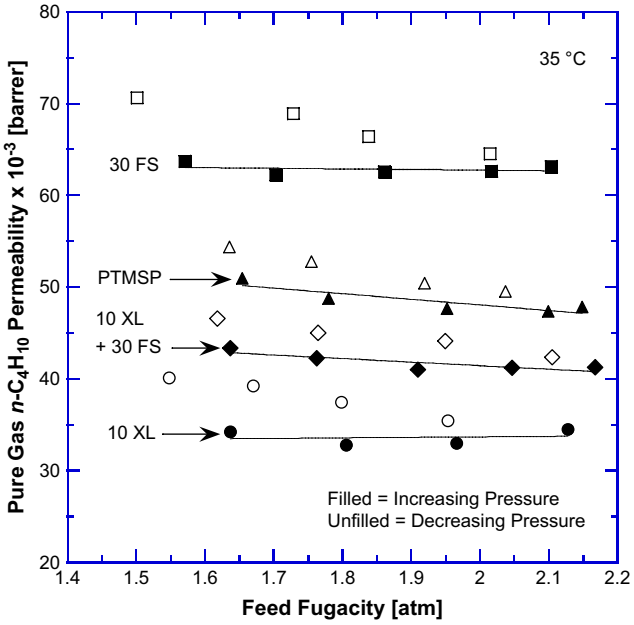

Fig. 1. Pure gas n-C_4H_{10} permeability coefficients of various PTMSP films at 35 °C. The solid lines are a linear fit to the data measured as feed pressure is increased, and these lines serve as a guide for the eye of the reader. All films were crosslinked at 180 °C in vacuum for 90 min, soaked in MeOH for 24 h, and then dried at ambient conditions for 72 h before permeability measurements began. The thickness of the films was approximately 100 μm. The labels are: uncrosslinked PTMSP (PTMSP), uncrosslinked PTMSP containing 30 wt% FS nanoparticles (30 FS), crosslinked PTMSP containing 10 wt% bis(azide) crosslinker (10 XL), and crosslinked PTMSP containing 10 wt% bis(azide) crosslinker and 30 wt% FS nanoparticles (10 XL + 30 FS). In this figure and in Figs. 2–5, filled data points correspond to measurements made as feed pressure was increased, and unfilled data points correspond to measurements made as feed pressure was decreased.

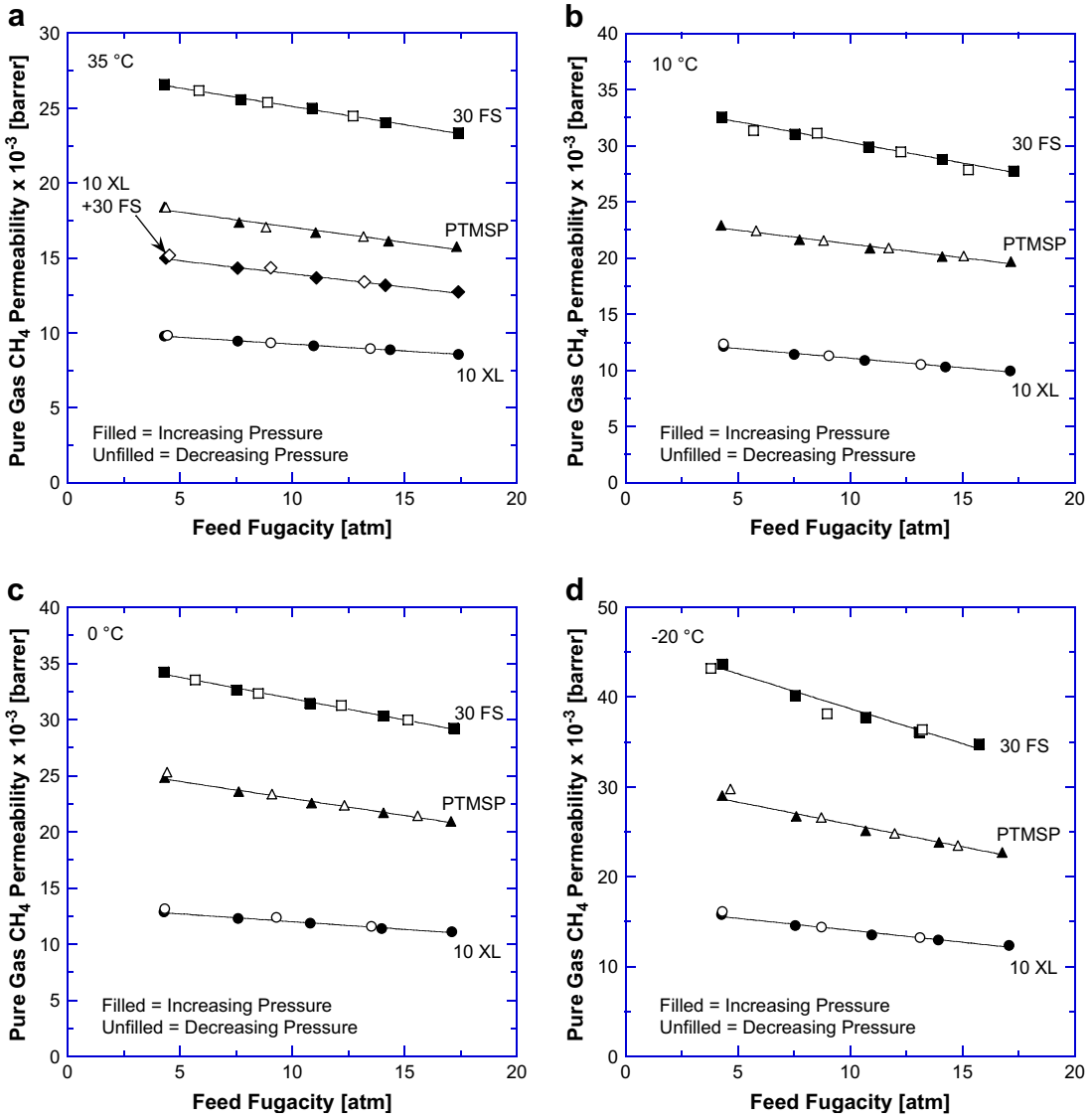

Fig. 2. Pure gas CH_4 permeability coefficients of various PTMSP films at (a) 35 °C, (b) 10 °C, (c) 0 °C, and (d) −20 °C. The solid lines are smooth fits to the data measured as the pressure is increased, and these lines serve as a guide for the eye of the reader. All films were crosslinked at 180 °C in vacuum for 90 min, soaked in MeOH for 24 h, and then dried at ambient conditions for 72 h before permeability measurements began. The thickness of the films was approximately 100 μm.

pump oil vapor was reduced by installing two liquid N_2 traps on the line between the vacuum pump and the vacuum oven. All films in this study were soaked in methanol (MeOH), which is a swelling non-solvent for PTMSP [29], for 24 h following film preparation and exposure to high temperatures under vacuum. Soaking the films in MeOH helps to prepare PTMSP samples with reproducible properties [29]. The length of the MeOH immersion allowed MeOH to reach equilibrium sorption in the films [29]. All films were dried at ambient conditions for 72 h after MeOH immersion, which allowed all MeOH to desorb from the films [29]. Afterwards, film thickness was measured, and transport property testing was started. Films used in pure gas permeation experiments were approximately 100 μm thick, while films used in mixed gas permeation experiments were approximately 500 μm thick.

3.3. Permeation measurements

3.3.1. Pure gas

Pure gas CH_4 and n-C_4H_{10} permeabilities were measured in a constant pressure, variable volume permeation cell. Once steady state was achieved, the permeability of gas A was evaluated using the following equation [3]:

$$P_A = \frac{1}{A} \times \frac{V}{t} \times \frac{l}{f_2 - f_1} \times \frac{273.15\ K}{T} \times \frac{p_a}{76} \times 10^{10} \quad (8)$$

where P_A is the permeability coefficient (barrer), A is the film area (cm^2), V is the volume of permeating gas (cm^3) collected during a time, t (s), l is film thickness (cm), f_2 is gas fugacity on the upstream (*i.e.*, high pressure) side of the film (cmHg), f_1 is the gas fugacity on the downstream (*i.e.*, low pressure) side of the film (cmHg), T is the measurement temperature (K), and p_a is atmospheric pressure (cmHg). The area of the films used in the pure gas permeation experiment was $13.8 \pm 0.2\ cm^2$, and the film thickness was 100 ± 10 μm. The downstream pressure in all cases was atmospheric.

3.3.2. Mixed gas

Mixed gas permeabilities were measured in a constant pressure, variable volume system connected to a gas chromatograph that was equipped with a thermal conductivity detector (TCD) and a flame ionization detector (FID) [14]. The permeate stream was swept from

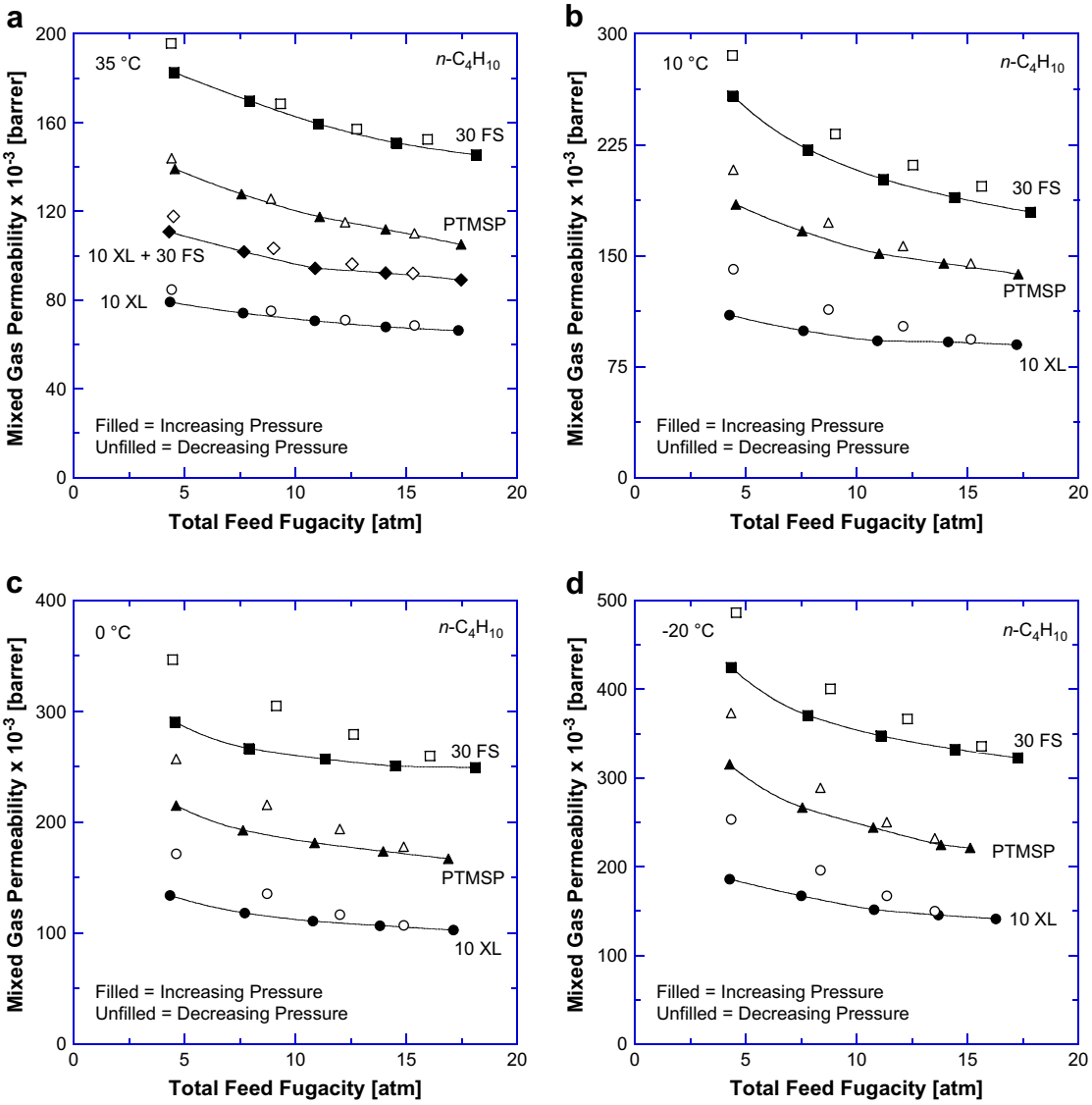

Fig. 3. Mixed gas n-C_4H_{10} permeabilities of various PTMSP films at (a) 35 °C, (b) 10 °C, (c) 0 °C, and (d) −20 °C. The solid lines are smooth fits to the data measured as the pressure is increased, and these lines serve as a guide for the eye of the reader. All films were crosslinked at 180 °C in vacuum for 90 min, soaked in MeOH for 24 h, and then dried at ambient conditions for 72 h before permeability measurements began. The thickness of the films was approximately 500 μm.

the low-pressure side of the film by Helium. The permeate concentration of gas A in the sweep, x_{1A}, and the sweep gas flow rate, S (cm^3/s) were measured, and the mixed gas permeability of gas A was calculated as follows [14]:

$$P_A = \frac{x_{1A} S l}{x_c^P A (f_{2A} - f_{1A})} \times \frac{273.15\,K}{T} \times \frac{p_a}{76} \times 10^{10} \quad (9)$$

where x_c^P is the mole fraction of sweep gas in the permeate stream, and f_{2A} and f_{1A} are the feed and permeate fugacities of gas A, respectively. The ratio of permeate to feed flow rate (*i.e.*, the stage cut) was always less than 1%, so the residue and feed gas compositions remain essentially equal [10]. The area of films used in the mixed gas experiments was 0.31 ± 0.01 cm^2, and the film thickness was 500 ± 40 μm. In mixed gas permeation experiments, the film area was less and film thickness was greater than that of the films used for pure gas permeation experiments. Decreasing film area and increasing film thickness reduced the amount of gas permeating across the film, thereby decreasing the flow rate of residue gas required to maintain the stage cut below 1%, which minimized the consumption of feed gas.

The pure gas CH_4 permeability was measured at 35 °C and 4.4 atm feed pressure at the beginning of each mixed gas experiment to confirm that each PTMSP film being tested had the same initial transport properties. The temperature of the cell was then adjusted to the required experimental temperature, and the gas mixture was introduced to the feed side of the film at 4.4 atm. For all experiments in this study, the mixed gas feed composition was 98 mol% CH_4 and 2 mol% n-C_4H_{10}. The mixed gas permeabilities were measured at 5 pressures as the feed (or upstream) pressure was increased to its maximum value, and at 4 pressures as the film was depressurized to atmospheric pressure. Permeability was measured as the film was depressurized to probe for any conditioning effects by the mixed gas feed on the polymer film. At each temperature considered, a new film was loaded into the mixed gas permeation cell, which minimized the hysteresis effects of previous permeability measurements.

For all PTMSP films and at all temperatures considered, pure gas CH_4 permeabilities measured in the mixed gas permeation cell agreed with those measured in the pure gas permeation cell. The thicknesses of the films in the pure gas permeation experiments (~100 μm) and mixed gas permeation experiments (~500 μm) are

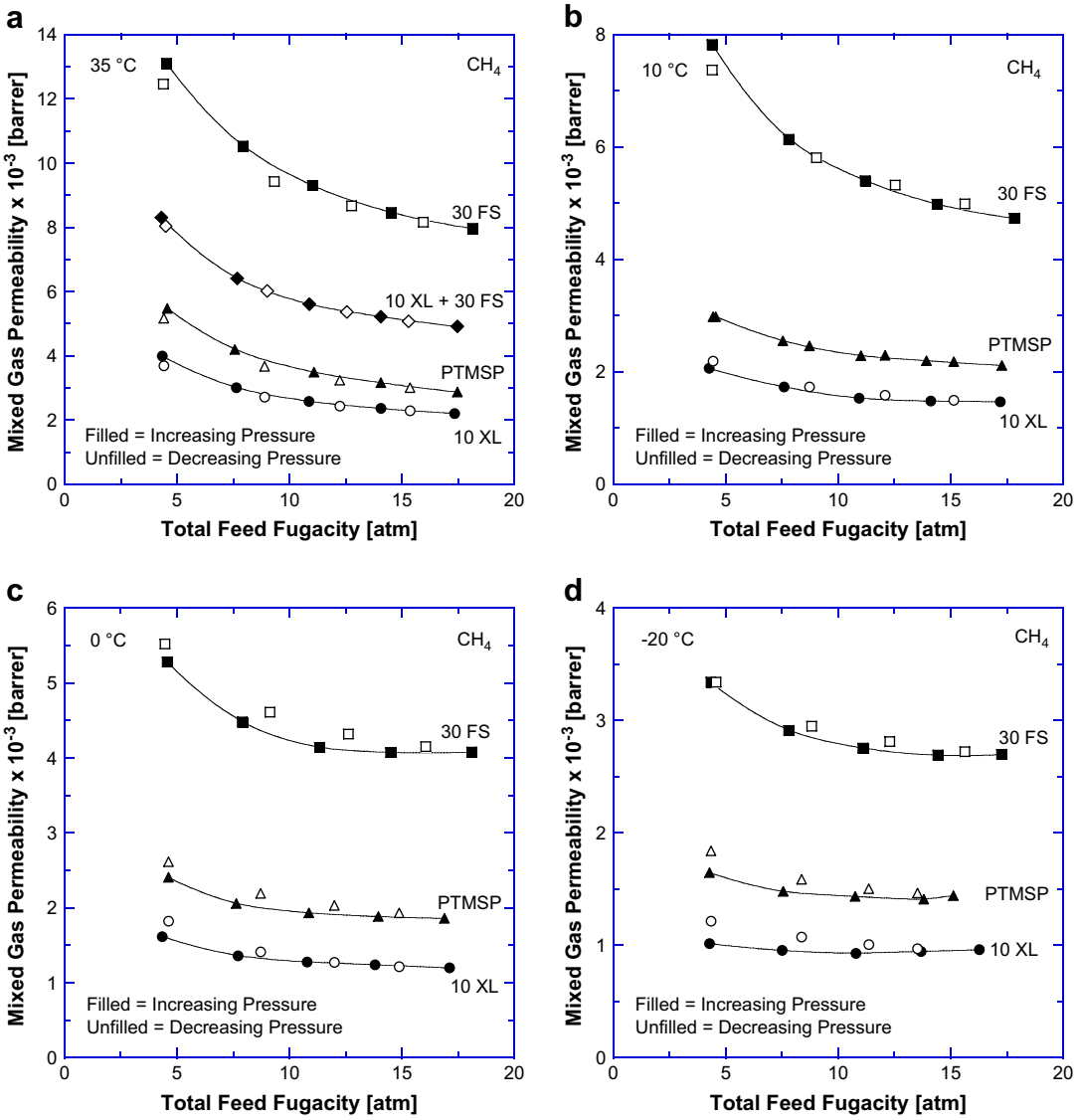

Fig. 4. Mixed gas CH_4 permeability of various PTMSP films at (a) 35 °C, (b) 10 °C, (c) 0 °C, and (d) −20 °C. The solid lines are smooth fits to the data measured as the pressure is increased, and these lines serve as a guide for the eye of the reader. All films were crosslinked at 180 °C in vacuum for 90 min, soaked in MeOH for 24 h, and then dried at ambient conditions for 72 h before permeability measurements began. The thickness of the films was approximately 500 μm.

different, and it has been reported that film thickness can affect the permeability of PTMSP [24,54]. However, no thickness dependence of pure and mixed gas permeabilities was observed for films in this study. This result could be caused by the fact that the films in this study were relatively thick and that the film thicknesses did not vary over as wide a range as in other studies where film thickness was shown to influence PTMSP permeabilities [24,54].

4. Results and discussion

4.1. Pure gas permeation

Fig. 1 presents pure gas n-C_4H_{10} permeabilities at 35 °C of uncrosslinked PTMSP, uncrosslinked PTMSP containing 30 wt% FS nanoparticles (30 FS), crosslinked PTMSP containing 10 wt% bis-(azide) crosslinker (10 XL), and crosslinked PTMSP containing 10 wt% bis(azide) crosslinker and 30 wt% FS nanoparticles (10 XL + 30 FS) as a function of n-C_4H_{10} fugacity at the upstream side of the film. The addition of crosslinks decreases permeability, and this decrease is consistent with the lower FFV of crosslinked material [33]. Upon addition of FS, the n-C_4H_{10} permeability increases by approximately 30%, relative to that of uncrosslinked PTMSP, and this increase is consistent with an increase in free volume caused by FS nanoparticles disrupting the polymer chain packing [10].

The n-C_4H_{10} permeability of all films is slightly higher when the permeability was measured as the film was depressurized (unfilled symbols in Fig. 1), which indicates slight conditioning of the films by n-C_4H_{10}. Conditioning occurs when penetrant sorption leads to dilation of the polymer sample as feed pressure is increased. In glassy polymers, the dilation of the sample may be slow to relax, resulting in films, when measured during depressurization, that have a slightly higher free volume than they had when the permeability measurement was made upon increasing feed pressure [56]. The increase in free volume upon depressurization often correlates with increased permeability [44]. Increases in the pure gas permeability of PTMSP upon depressurization have been reported for C_2H_6 [42], C_3H_8 [42], C_3F_8 [41] and ethylbenzene [40].

Fig. 2 presents pure gas CH_4 permeabilities as a function of upstream CH_4 fugacity. The permeabilities are presented at 35 °C, 10 °C, 0 °C, and −20 °C. At all temperatures, the permeability of the

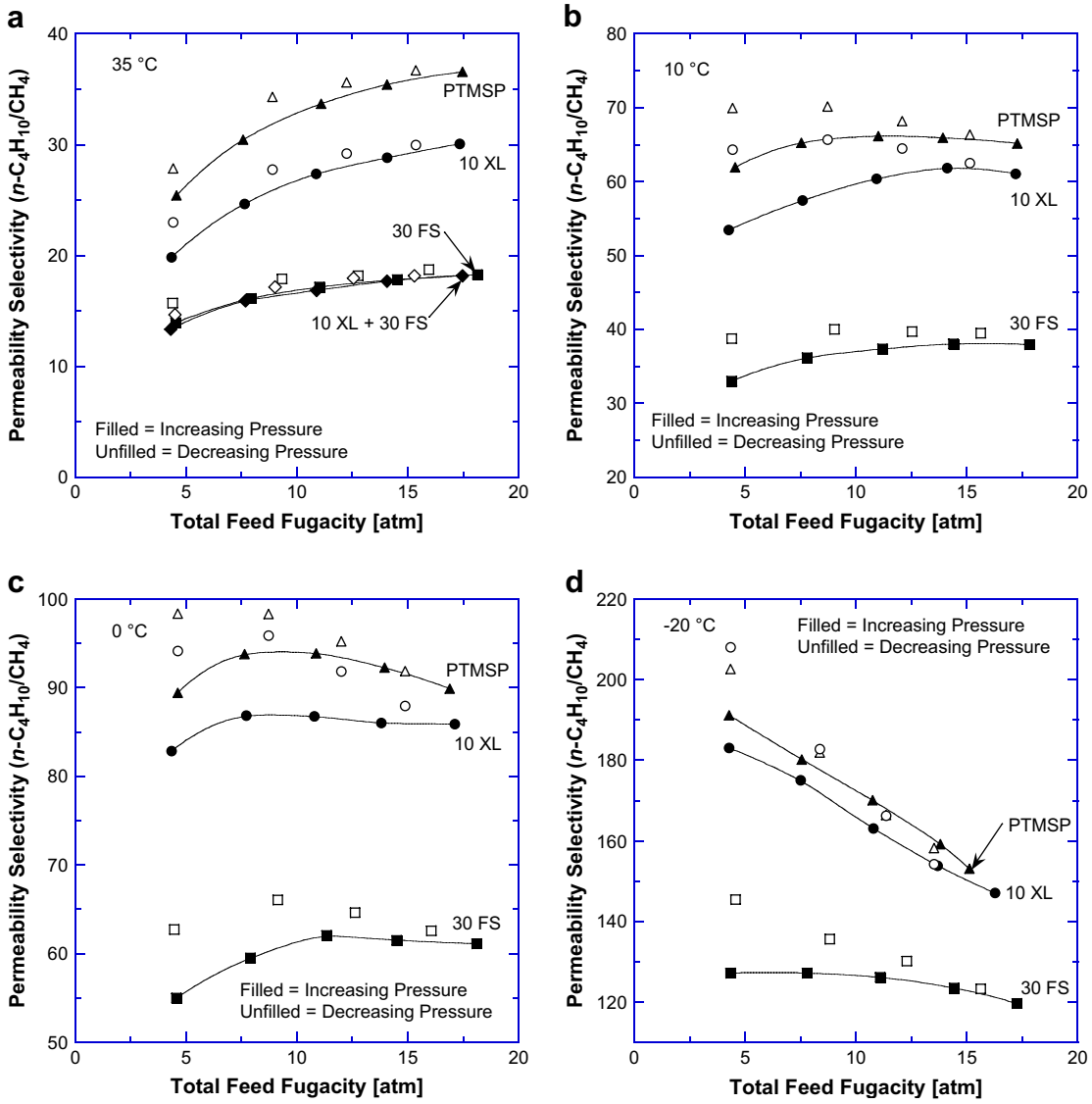

Fig. 5. Mixed gas n-C_4H_{10}/CH_4 permeability selectivity of various PTMSP films at (a) 35 °C, (b) 10 °C, (c) 0 °C, and (d) −20 °C. The solid lines are smooth fits to the data measured as the pressure is increased, and these lines serve as a guide for the eye of the reader. All films were crosslinked at 180 °C in vacuum for 90 min, soaked in MeOH for 24 h, and then dried at ambient conditions for 72 h before permeability measurements began. The thickness of the films was approximately 500 μm.

crosslinked film is lower than that of its uncrosslinked analog, presumably due to the lower FFV in crosslinked samples [33]. The addition of 30 wt% FS nanoparticles increases the permeability of both uncrosslinked PTMSP and crosslinked PTMSP by approximately 50%, relative to their unfilled analogs, and the permeability increase is qualitatively consistent with FS nanoparticles disrupting the polymer chain packing, thereby increasing the free volume of the resulting nanocomposites [10]. In this regard, the increases in CH_4 and n-C_4H_{10} permeabilities upon addition of 30 wt% FS are similar to those reported by De Sitter et al. [37], and Merkel et al. [10]. Therefore, the dispersion of FS nanoparticles in the PTMSP films in this study should be similar to that observed by De Sitter et al. [37], and Merkel et al. [10], where FS nanoparticles where observed to be aggregated in agglomerates in the size range of several hundred nanometers [10,37].

As shown in Fig. 2, the increase in pure gas CH_4 permeability due to 30 wt% FS addition is greater than the increase observed in pure gas n-C_4H_{10} permeability when FS is added to the film. A similar result was found by Merkel et al., where the pure gas CH_4 permeability of PTMSP increased by 60% when 40 wt% FS nanoparticles were added to PTMSP, while the pure gas n-C_4H_{10} permeability increased by 35% [10]. These results follow a trend where the increase in PTMSP permeability due to FS addition is less for larger molecules. This finding is consistent with transport mechanisms other than solution-diffusion (such as Knudsen flow in the extra free volume introduced by FS addition, which would preferentially increase the permeability of smaller molecules such as CH_4 [10]), beginning to play a role in the permeability properties of the nanocomposite films.

The relative decrease in CH_4 permeabilities with increasing feed fugacity is similar for all films in Fig. 2, and this decrease is slightly greater at −20 °C than at other temperatures. This decrease in permeability with increasing fugacity is attributed to the decrease in CH_4 solubility coefficients as fugacity increases [33,42,57]. At all temperatures, CH_4 permeabilities measured as the films were depressurized lie on the same trend lines as the CH_4 permeabilities measured while feed pressure was increased. Therefore, no conditioning is observed for CH_4, suggesting that CH_4 does not sorb enough to cause disruption in polymer chain packing that would be associated with conditioning [56].

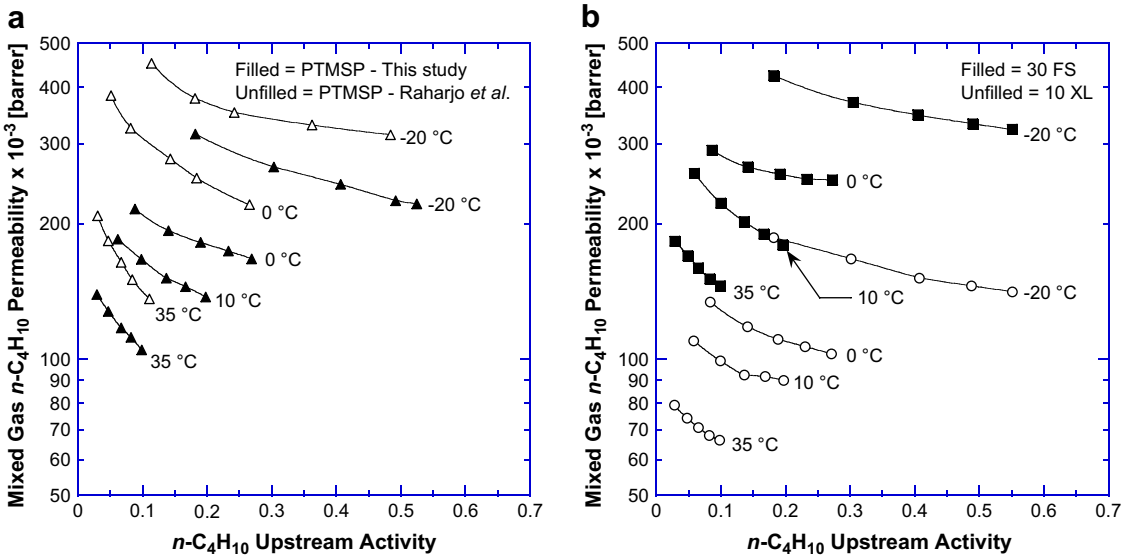

Fig. 6. Mixed gas n-C_4H_{10} permeabilities of (a) uncrosslinked PTMSP, and (b) PTMSP + 30 wt% FS (30 FS) and PTMSP + 10 wt% XL (10 XL) as a function of upstream n-C_4H_{10} activity. The smooth lines are intended to act as guides for the eye of the reader. The mixed gas n-C_4H_{10} permeabilities from this study are reported at 35 °C, 10 °C, 0 °C, and −20 °C. The mixed gas n-C_4H_{10} permeabilities from Raharjo et al. study are reported at 35 °C, 0 °C, and −20 °C [22]. n-C_4H_{10} activity is calculated as f_2/f_{sat}, where the fugacity value at saturation, f_{sat}, was calculated as described by Raharjo et al. [45].

4.2. Mixed gas permeation

4.2.1. Effect of crosslinking and FS nanoparticle addition

Fig. 3 presents mixed gas n-C_4H_{10} permeabilities of the PTMSP films considered in this study. The crosslinked unfilled (10 XL) and nanocomposite (10 XL + 30 FS) samples are about 40% less permeable to n-C_4H_{10} than their uncrosslinked analogs (PTMSP and 30 FS, respectively) at 35 °C, which is consistent with lower free volume in the crosslinked samples [33]. This decrease in permeability is similar at all temperatures for the unfilled crosslinked samples (10 XL). The addition of 30 wt% FS nanoparticles increases the mixed gas permeability coefficients at all temperatures, and this permeability increase is ascribed to FS nanoparticles disrupting chain packing, which increases free volume [10]. The addition of 30 wt% FS nanoparticles increases mixed gas n-C_4H_{10} permeabilities of both uncrosslinked and crosslinked samples by approximately 30%, which is similar to the increase in pure gas n-C_4H_{10} permeability observed in Fig. 1 when 30 wt% FS was added to uncrosslinked PTMSP and crosslinked PTMSP.

The mixed gas n-C_4H_{10} permeabilities presented in Fig. 3 decrease with increasing upstream fugacity. There is no significant difference in the relative decrease of n-C_4H_{10} permeabilities for different PTMSP films, and there is no qualitative difference observed when temperature decreases. Raharjo et al. also observed similar decreases in n-C_4H_{10} permeabilities in uncrosslinked PTMSP [22] and ascribed the decrease to a reduction in the mixed gas n-C_4H_{10} solubility coefficient as n-C_4H_{10} fugacity increased [22,57].

As shown in Fig. 3, mixed gas n-C_4H_{10} permeabilities were measured as the films were depressurized to investigate conditioning effects. At all temperatures, the n-C_4H_{10} permeabilities measured as the films were depressurized were equal to or greater than the mixed gas n-C_4H_{10} permeabilities measured as feed

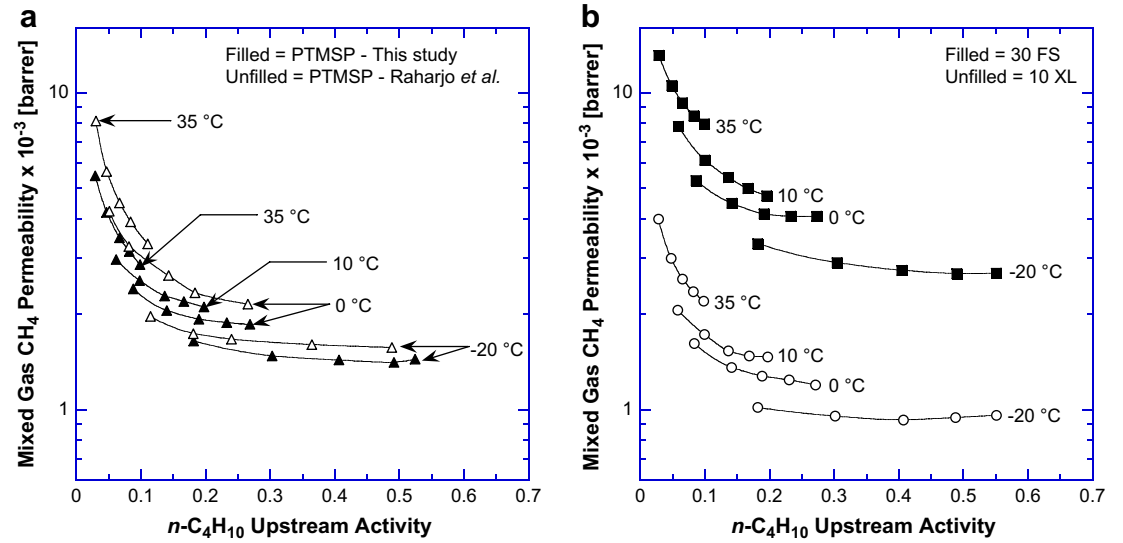

Fig. 7. Mixed gas CH_4 permeabilities of (a) uncrosslinked PTMSP, and (b) PTMSP + 30 wt% FS (30 FS) and PTMSP + 10 wt% XL (10 XL) as a function of upstream n-C_4H_{10} activity. The smooth lines are intended to act as guides for the eye of the reader. The mixed gas CH_4 permeabilities from this study are reported at 35 °C, 10 °C, 0 °C, and −20 °C. The mixed gas CH_4 permeabilities from Raharjo et al. study are reported at 35 °C, 0 °C, and −20 °C [22].

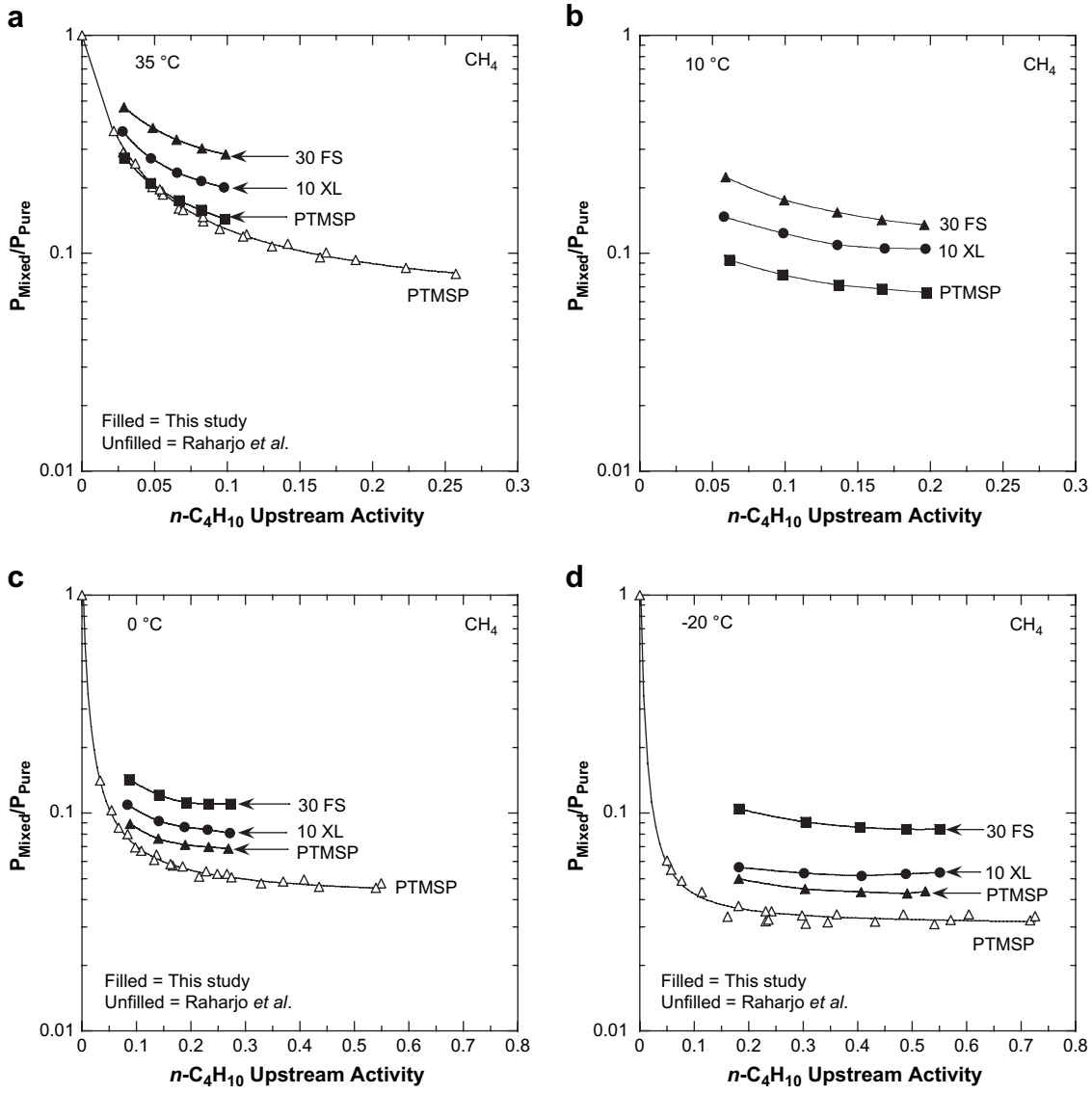

Fig. 8. The ratio of mixed gas CH_4 permeabilities to pure gas CH_4 permeabilities at infinite dilution as a function of upstream n-C_4H_{10} activity at (a) 35 °C, (b) 10 °C, (c) 0 °C, and (d) −20 °C. The filled symbols represent values from this study, while the unfilled symbols represent data from Raharjo et al., who reports such data for unfilled uncrosslinked PTMSP [22,59].

pressure was increased. At any given feed fugacity and temperature for any of the films (*i.e.*, PTMSP, 10 XL, and 30 FS), the relative change in mixed gas n-C_4H_{10} permeabilities between pressurization and depressurization is similar. Therefore, the addition of crosslinks or FS does not change the relative degree of conditioning. At 10 °C, 0 °C, and −20 °C there are significant increases in mixed gas n-C_4H_{10} permeabilities when the films were depressurized, and the increases are more significant when the temperature and upstream gas fugacity were lower. At 35 °C, the increases in mixed gas n-C_4H_{10} permeabilities for all films upon depressurization are not significant within the resolution of the experiment. The negligible change in mixed gas n-C_4H_{10} permeabilities on depressurization at 35 °C may be a consequence of lower n-C_4H_{10} activities in the mixed gas feed stream at higher temperatures. At higher activities, penetrants sorb to a greater extent, thereby dilating the polymer and disrupting polymer chain packing to a greater degree [56], causing a greater increase in conditioning effects.

Fig. 4 presents mixed gas CH_4 permeabilities of various PTMSP films as a function of total upstream fugacity. The addition of crosslinks decreases mixed gas CH_4 permeabilities of PTMSP, while the addition of FS nanoparticles increases mixed gas CH_4 permeabilities, similar to the trends observed in the pure gas case (*cf.*, Fig. 2). The decrease in mixed gas CH_4 permeability of the unfilled samples upon crosslinking is approximately 30% at all temperatures. The decrease in mixed gas CH_4 permeability in the nanocomposite sample at 35 °C upon crosslinking is approximately 40%. The mixed gas CH_4 permeability of uncrosslinked PTMSP and crosslinked PTMSP increases by 100–130% due to addition of 30 wt% FS. This increase is substantially greater than the 40% increase in mixed gas n-C_4H_{10} permeability in both uncrosslinked and crosslinked films when FS nanoparticles were added.

As shown in Fig. 4, there is at most only slight difference in the mixed gas CH_4 permeabilities measured during pressurization and depressurization. Therefore, any conditioning that is occurring has weak affect on CH_4 permeability. The uncertainty in the mixed gas CH_4 permeabilities measured during depressurization is approximately ±5%.

Fig. 5 presents the mixed gas n-C_4H_{10}/CH_4 selectivities of various PTMSP films as a function of total feed fugacity. At all temperatures, the mixed gas n-C_4H_{10}/CH_4 selectivities decrease when PTMSP is

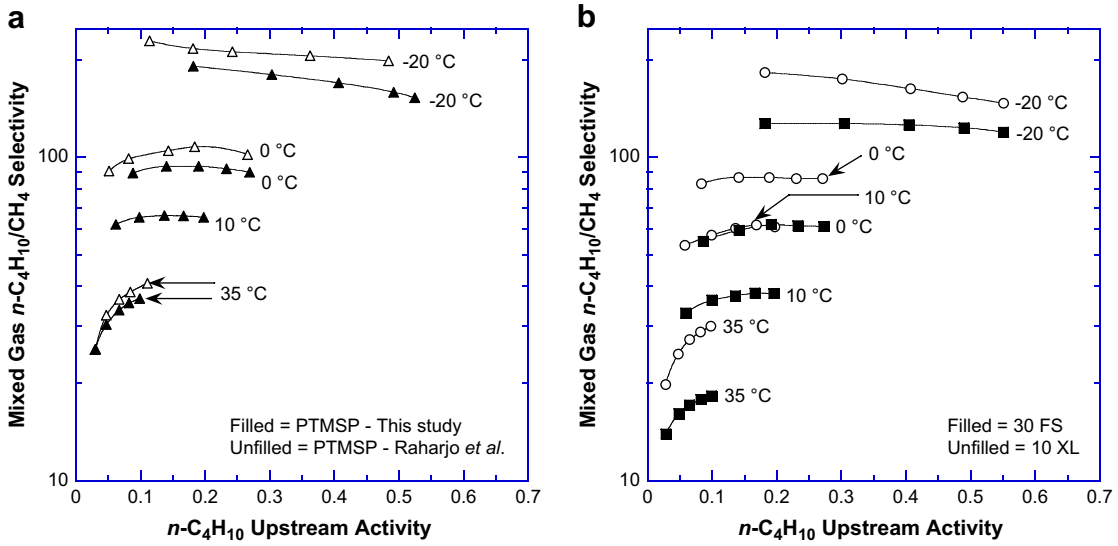

Fig. 9. Mixed gas n-C_4H_{10}/CH_4 selectivities of (a) uncrosslinked PTMSP, and (b) PTMSP + 30 wt% FS (30 FS) and PTMSP + 10 wt% XL (10 XL) as a function of upstream n-C_4H_{10} activity. The smooth lines are intended to act as guides for the eye of the reader. The mixed gas n-C_4H_{10}/CH_4 selectivities from this study are reported at 35 °C, 10 °C, 0 °C, and −20 °C. The mixed gas n-C_4H_{10}/CH_4 selectivities from Raharjo et al. study are reported at 35 °C, 0 °C, and −20 °C [22].

crosslinked (*e.g.*, compare PTMSP to 10 XL in Fig. 5), which is consistent with previous results [33]. The addition of FS causes a substantial decrease in mixed gas selectivity (*e.g.*, compare PTMSP to 30 FS in Fig. 5), which is consistent with previous results [10,33]. For example, at 35 °C, the mixed gas n-C_4H_{10}/CH_4 selectivities of 30 FS are approximately 50% less than those of PTMSP, while at −20 °C a 30% decrease in mixed gas selectivity is observed.

Crosslinking PTMSP decreases its FFV [33], so the crosslinked films are likely to be more size-sieving than their uncrosslinked analogs [44], which would favor a reduction in the mixed gas n-C_4H_{10}/CH_4 permeability selectivity upon crosslinking. When FS is added to PTMSP, the decrease in mixed gas n-C_4H_{10}/CH_4 selectivities is thought to be caused by FS-induced creation of structures (*e.g.*, pores large enough to permit Knudsen flow) that are CH_4 selective [10]. In the case of crosslinking and addition of FS, the overall effect is a reduction in the mixed gas n-C_4H_{10}/CH_4 permeability selectivity, but the molecular basis for this effect is probably different for crosslinking and FS addition.

As shown in Fig. 5, when temperature decreases, the mixed gas permeability selectivities of crosslinked PTMSP (10 XL) and nanocomposite uncrosslinked PTMSP (30 FS) become more comparable to the selectivities of uncrosslinked PTMSP. This effect could be caused by the increase in n-C_4H_{10} activity in the feed gas as temperature decreases. At higher activities more n-C_4H_{10} sorbs in the films and can block the permeation of CH_4. Higher concentrations of n-C_4H_{10} may reduce the effect that crosslinks and FS addition have on decreasing mixed gas n-C_4H_{10}/CH_4 permeability selectivity. However, a complete explanation of this phenomenon is not currently available. The shape of the permeability versus fugacity plots changes with temperature, and the reason for this will be discussed in greater detail below.

The mixed gas n-C_4H_{10}/CH_4 selectivities were also measured as the films were depressurized, and these values are displayed as the unfilled symbols in Fig. 5. At 10 °C, 0 °C, and −20 °C, the mixed gas n-C_4H_{10}/CH_4 selectivities measured during depressurization are greater than those measured as the films were pressurized, and the difference is most significant at the lowest fugacities. In contrast, at 35 °C, there was no significant increase in mixed gas selectivity upon depressurization. For all films, and at all temperatures, the relative increase in mixed gas selectivity upon depressurization is similar. The increase in mixed gas n-C_4H_{10}/CH_4 selectivities upon depressurization is a consequence of the mixed gas n-C_4H_{10} permeabilities increasing significantly more than the mixed gas CH_4 permeabilities during depressurization, as shown in Figs. 3 and 4. That is, conditioning influences the permeation properties of the larger penetrant (n-C_4H_{10}) more than that of the smaller penetrant (CH_4).

4.2.2. Effect of upstream activity

Fig. 6 presents mixed gas n-C_4H_{10} permeabilities of various PTMSP films as a function of n-C_4H_{10} upstream activity and temperature. The mixed gas n-C_4H_{10} permeabilities of all films decrease as n-C_4H_{10} activity increases, which is consistent with the decrease in n-C_4H_{10} solubility coefficients with increasing n-C_4H_{10} activity observed in pure gas sorption studies [33,42,57]. The mixed gas n-C_4H_{10} permeabilities increase as temperature decreases, which agrees with prior reports of negative activation energies of permeation for gases and vapors in PTMSP [10,58]. Similar trends in mixed gas n-C_4H_{10} permeability were reported by Raharjo et al. [22], and data from their study are presented in Fig. 6 for comparison. At similar temperature and activity, the mixed gas n-C_4H_{10} permeabilities of uncrosslinked PTMSP in this study are slightly less than those reported by Raharjo et al., and this variation can be explained by differences in the thermal histories of the films in each study. All films in this study were thermally annealed at 180 °C in a vacuum oven for 90 min, while films in the Raharjo et al. study were not subjected to any thermal treatment [22]. The thermal annealing treatment decreases pure gas CH_4 permeabilities and increases the density of PTMSP [44]. For example, the uncrosslinked PTMSP films in this study had a density of 0.76 ± 0.01 g/cm^3, and a pure gas CH_4 permeability at 35 °C and 4.4 atm of 18,000 barrer. In the Raharjo et al. study, the density of PTMSP was 0.73 ± 0.01 g/cm^3, and the pure gas CH_4 permeability at 35 °C and 4.4 atm was 26,000 barrer [22]. Therefore, the thermal annealing treatment used in this study is believed to be the basis for differences in n-C_4H_{10} permeabilities between this study and that of Raharjo et al.

Fig. 7 presents mixed gas CH_4 permeabilities of various PTMSP films as a function of temperature and upstream n-C_4H_{10} activity. The mixed gas CH_4 permeabilities from Raharjo et al. [22] are slightly greater than those of the uncrosslinked PTMSP films in this study, and this difference is related to differences in thermal

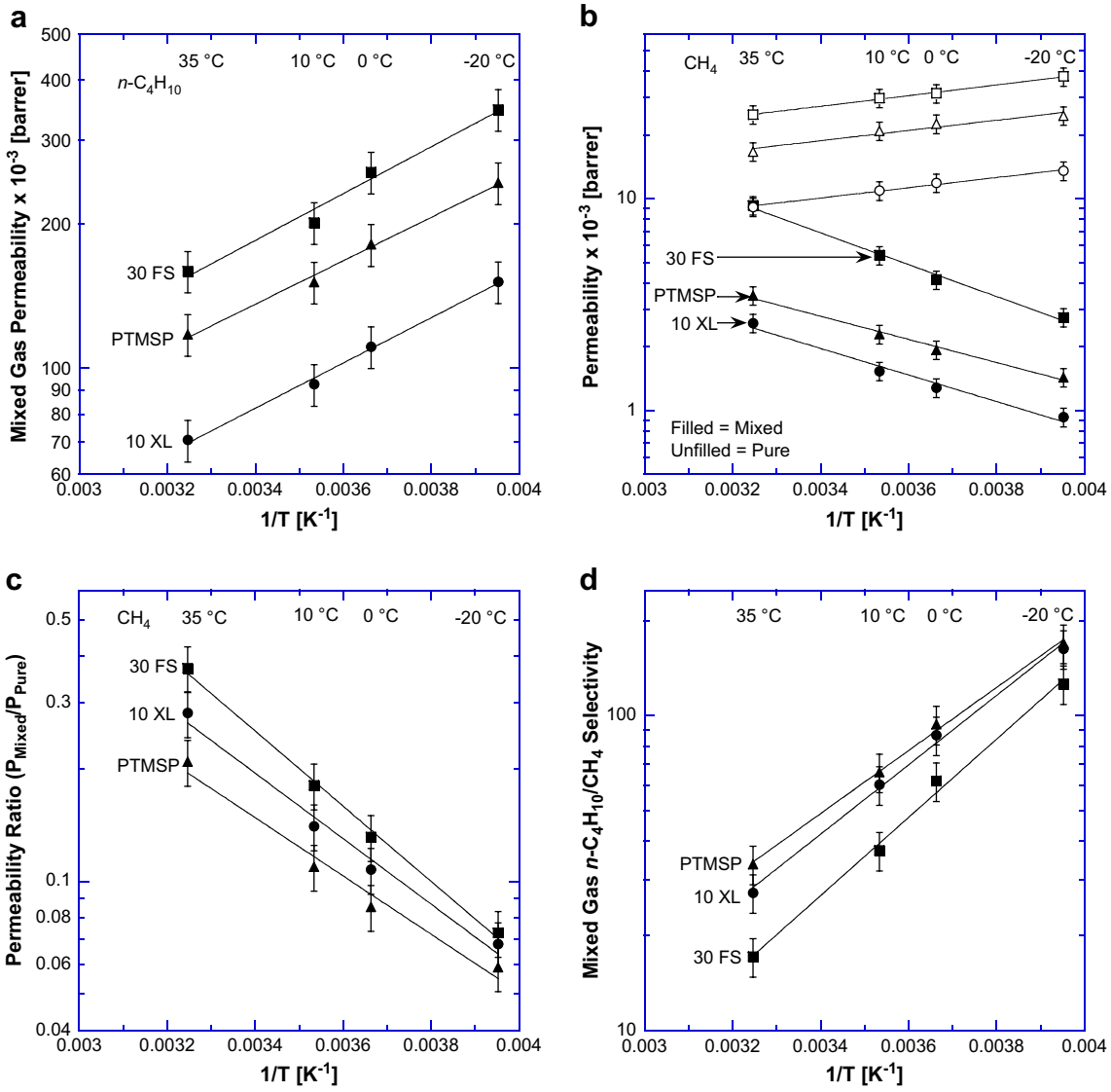

Fig. 10. The effect of temperature on (a) mixed gas n-C_4H_{10} permeabilities, (b) mixed gas CH_4 permeabilities, (c) the ratio of mixed to pure gas CH_4 permeabilities, and (d) mixed gas n-C_4H_{10}/CH_4 selectivities of various PTMSP films. The data are reported at a CH_4 feed fugacity of 11 atm (*i.e.*, the total feed fugacity was approximately 11.2 atm in the mixed gas experiments) for measurements made as the film was pressurized. The solid lines are an Arrhenius fit to the data. All films were crosslinked at 180 °C in vacuum for 90 min, soaked in MeOH for 24 h, and then dried at ambient conditions for 72 h before permeability measurements began.

histories of the films. The mixed gas CH_4 permeabilities of all films decrease as n-C_4H_{10} upstream activity increases. For all films, the mixed gas CH_4 permeabilities decrease with decreasing temperature, and this result is opposite to the behavior observed for pure gas CH_4 permeation in PTMSP, where CH_4 permeability increases with decreasing temperature [10,22,42,58]. This interesting trend results from a competition among several factors. As temperature decreases, CH_4 solubility would, in the absence of n-C_4H_{10}, increase more than the CH_4 diffusion coefficient decreases, resulting in an increase in CH_4 permeability [22,42,57,58]. However, in the presence of n-C_4H_{10}, as temperature decreases, the amount of n-C_4H_{10} sorbed in the film, at fixed activity, increases and, due to the resulting competitive sorption effects, the CH_4 solubility actually decreases (rather than increases) [57]. As temperature decreases, CH_4 diffusivity decreases in both pure gas and mixed gas cases [22,42,58]. However, in the presence of n-C_4H_{10} at fixed activity, the decrease in CH_4 diffusivity with temperature is greater than in the absence of n-C_4H_{10} [22]. Consequently, the CH_4 permeability, in the presence of n-C_4H_{10}, decreases as temperature decreases, but, in the absence of n-C_4H_{10}, the CH_4 permeability increases as temperature decreases (*cf.*, Fig. 2).

Fig. 8 presents CH_4 blocking ratios (*i.e.*, the ratio of mixed gas CH_4 permeabilities to pure gas CH_4 permeabilities) as a function of upstream n-C_4H_{10} activity. The ratios of the mixed to pure gas CH_4 permeabilities of uncrosslinked unfilled PTMSP are similar to the values reported by Raharjo et al. [22,59]. At all temperatures, the ratios of mixed to pure gas CH_4 permeabilities are greater for crosslinked PTMSP (10 XL) and nanocomposite uncrosslinked PTMSP (30 FS) than for uncrosslinked PTMSP. This increase is thought to be caused by crosslinks and FS nanoparticles changing the free volume characteristics of PTMSP such that the blocking of CH_4 permeation by n-C_4H_{10} is reduced in the 10 XL and 30 FS samples.

Fig. 9 presents the mixed gas n-C_4H_{10}/CH_4 selectivities of various PTMSP films as a function of n-C_4H_{10} activity and temperature. Some of these data were presented earlier in Fig. 5, but the shape of the selectivity versus fugacity was not discussed at that point. The n-C_4H_{10}/CH_4 selectivities of all films increase as temperature

decreases. This increase occurs because mixed gas n-C_4H_{10} permeabilities increase with decreasing temperature, while mixed gas CH_4 permeabilities decrease with decreasing temperature (*cf.*, Figs. 6 and 7). At 35 °C, the n-C_4H_{10}/CH_4 selectivities increase with increasing n-C_4H_{10} activity. For example, the n-C_4H_{10}/CH_4 selectivity of uncrosslinked PTMSP increases from 25 to 36 when n-C_4H_{10} activity increases from 0.03 to 0.10. This increase in selectivity occurs because, over this activity range, CH_4 permeability is decreasing faster than that of n-C_4H_{10} with increasing activity [22]. At all temperatures other than −20 °C, the n-C_4H_{10}/CH_4 selectivities are relatively constant when n-C_4H_{10} activity is greater than about 0.15, because at higher activity values, the blocking of CH_4 transport by n-C_4H_{10} reaches an asymptote. At 0 °C and 10 °C, a significant increase in n-C_4H_{10}/CH_4 selectivity with increasing activity is not observed because the lowest activity value that was experimentally accessible was probably in a range where blocking had already reached its asymptotic value. At −20 °C, n-C_4H_{10}/CH_4 selectivity decreases slightly with increasing activity, and this result is consistent with the findings of Raharjo et al. [22].

4.2.3. Effect of temperature

Fig. 10 presents the effect of temperature on the mixed gas transport properties of various PTMSP films. All mixed and pure gas permeabilities and selectivities are reported for an upstream CH_4 fugacity of 11 atm, which was selected because it provides a convenient reference point for comparison with pure gas CH_4 data in Fig. 2. In Fig. 10a, the mixed gas n-C_4H_{10} permeabilities increase as temperature decreases, and the data follow Eq. (6). The activation energies of n-C_4H_{10} permeation were calculated using Eq. (6). The addition of crosslinks or nanoparticles to PTMSP did not change the temperature dependence of the mixed gas n-C_4H_{10} permeation. For all films in this study, the activation energy of mixed gas n-C_4H_{10} permeation is -9 ± 1 kJ/mol.

The activation energies of pure and mixed gas CH_4 permeation are calculated from the data presented in Fig. 10b, and the values are recorded in Table 1. For all films, the pure gas activation energies are negative, while the activation energies of mixed gas CH_4 permeation are positive. The activation energies of pure gas CH_4 permeation are similar for all films. Likewise, the activation energies of mixed gas CH_4 permeation are similar for all films. As indicated earlier, the presence of n-C_4H_{10} in the feed gas has a profound influence on CH_4 permeation properties, and the activation energy data are one further example of this phenomenon.

In Fig. 10c, the ratios of mixed to pure gas CH_4 permeabilities are observed to decrease as temperature decreases. This decrease could be related to the activity of n-C_4H_{10} in the feed gas in the mixed gas permeation experiments. When the fugacity is fixed, as it is for the data reported in Fig. 10c, the activity of n-C_4H_{10} in the feed gas increases as temperature decreases. Consequently, more n-C_4H_{10} is present at lower temperatures in the PTMSP films to block the permeation of CH_4 [22], which results in lower mixed gas CH_4 permeabilities, and lower mixed to pure gas CH_4 permeability ratios.

The mixed gas n-C_4H_{10}/CH_4 selectivities of all PTMSP films shown in Fig. 10d are observed to increase as temperature decreases. The reason for the increase in selectivity is caused by n-C_4H_{10} permeabilities increasing and CH_4 permeabilities decreasing when temperature decreases (*cf.*, Figs. 6 and 7). At all temperatures, the mixed gas selectivities of crosslinked PTMSP films and nanocomposite uncrosslinked PTMSP films are less than that of the uncrosslinked PTMSP films.

Table 1
Activation energies of pure and mixed gas CH_4 permeation in various PTMSP films

Film	E_p (kJ/mol) – pure gas	E_p (kJ/mol) – mixed gas
PTMSP	-4.6 ± 1.0	11 ± 1
10 XL	-4.6 ± 1.0	12 ± 1
30 FS	-4.8 ± 1.0	14 ± 1

The activation energies are reported at a CH_4 fugacity of 11 atm in the feed gas.

5. Conclusions

PTMSP was crosslinked with a bis(azide) crosslinker. Crosslinked PTMSP was insoluble in toluene, cyclohexane, and tetrahydrofuran, all of which are good solvents for uncrosslinked PTMSP. The addition of crosslinks to PTMSP decreased the mixed gas CH_4 and n-C_4H_{10} permeabilities, and the decrease was consistent with a decrease in FFV of crosslinked PTMSP. FS nanoparticle addition to uncrosslinked PTMSP and crosslinked PTMSP increased the mixed gas CH_4 and n-C_4H_{10} permeabilities, as FS nanoparticles are thought to disrupt the polymer chain packing, causing additional free volume to be created.

The mixed gas n-C_4H_{10}/CH_4 selectivities of crosslinked PTMSP and nanocomposite PTMSP were less than those of uncrosslinked PTMSP. Crosslinking PTMSP decreases FFV. Consequently, CH_4 permeability is reduced less by crosslinking than n-C_4H_{10} permeability. In samples containing FS, enough free volume is added to permit the onset of transport mechanisms that are CH_4 selective. Consequently, n-C_4H_{10}/CH_4 selectivity decreases in samples containing FS. As temperature decreased, mixed gas n-C_4H_{10} permeabilities increased, while mixed gas CH_4 permeabilities decreased. Overall, n-C_4H_{10}/CH_4 permeability selectivities increase with decreasing temperature. The decrease in mixed gas CH_4 permeability with decreasing temperature is opposite to that observed for pure gas CH_4 permeation, where an increase in permeability is observed with decreasing temperature. This difference in behavior is thought to be related to the blocking of CH_4 permeation by n-C_4H_{10} in the gas mixture.

Acknowledgements

We gratefully acknowledge partial support of this work by the U.S. Department of Energy (DE-FG03-02ER15362) and the National Science Foundation (CBET-0515425)

References

[1] Baker RW. Future directions of membrane gas separation technology. Industrial and Engineering Chemistry Research 2002;41:1393–411.
[2] Freeman BD, Pinnau I. In: Freeman BD, Pinnau I, editors. Polymer membranes for gas and vapor separation: chemistry and materials science. ACS symposium series; 1999. p. 1–27.
[3] Ghosal K, Freeman BD. Gas separation using polymer membranes: an overview. Polymers for Advanced Technologies 1994;5:673–97.
[4] Schultz J, Peinemann KV. Membranes for separation of higher hydrocarbons from methane. Journal of Membrane Science 1996;110:37–45.
[5] Spillman RW. Economics of gas separation membranes. Chemical Engineering Progress 1989;85:41–62.
[6] Pinnau I, Casillas CG, Morisato A, Freeman BD. Hydrocarbon/hydrogen mixed gas permeation in poly[1-(trimethylsilyl)-1-propyne] (PTMSP), poly(1-phenyl-1-propyne) (PPP), and PTMSP/PPP blends. Journal of Polymer Science, Part B: Polymer Physics 1996;34:2613–21.
[7] Pinnau I, Casillas CG, Morisato A, Freeman BD. Long-term permeation properties of poly[1-(trimethylsilyl)-1-propyne] membranes in hydrocarbon-vapor environment. Journal of Polymer Science, Part B: Polymer Physics 1997;35:1483–90.
[8] Pinnau I, Toy LG. Transport of organic vapors through poly[1-(trimethylsilyl)-1-propyne]. Journal of Membrane Science 1996;116:199–209.
[9] Teplyakov VV, Roizard D, Favre E, Khotimsky VS. Investigations on the peculiar permeation properties of volatile organic compounds and permanent gases through PTMSP. Journal of Membrane Science 2003;220:165–75.
[10] Merkel TC, He Z, Pinnau I, Freeman BD, Meakin P, Hill AJ. Effect of nanoparticles on gas sorption and transport in poly[1-(trimethylsilyl)-1-propyne]. Macromolecules 2003;36:6844–55.
[11] Masuda T, Isobe E, Higashimura T, Takada K. Poly[1-(trimethylsilyl)-1-propyne]: a new high polymer synthesized with transition-metal catalysts and characterized by extremely high gas permeability. Journal of the American Chemical Society 1983;105:7473–4.

[12] Nagai K, Masuda T, Nakagawa T, Freeman BD, Pinnau I. Poly[1-(trimethylsilyl)-1-propyne] and related polymers: synthesis, properties and functions. Progress in Polymer Science 2001;26:721–98.
[13] Srinivasan R, Auvil SR, Burban PM. Elucidating the mechanism(s) of gas transport in poly[1-(trimethylsilyl)-1-propyne] (PTMSP) membranes. Journal of Membrane Science 1994;86:67–86.
[14] Merkel TC, Gupta RP, Turk BS, Freeman BD. Mixed-gas permeation of syngas components in poly(dimethylsiloxane) and poly[1-(trimethylsilyl)-1-propyne] at elevated temperatures. Journal of Membrane Science 2001;191:85–94.
[15] Nakagawa T, Fujisaki S, Nakano H, Higuchi A. Physical modification of poly[1-(trimethylsilyl)-1-propyne] membranes for gas separation. Journal of Membrane Science 1994;94:183–93.
[16] Ash R, Barber RM, Pope CG. Flow of adsorbable gases and vapors in a microporous medium. II. Binary mixtures. Proceedings of the Royal Society of London 1963;271:19–33.
[17] Ash R, Barrer RM, Lowson RT. Transport of single gases and of binary gas mixtures in a microporous carbon membrane. Journal of the Chemical Society, Faraday Transactions 1: Physical Chemistry in Condensed Phases 1973;69:2166–78.
[18] Ash R, Barrer RM, Sharma P. Sorption and flow of carbon dioxide and some hydrocarbons in a microporous carbon membrane. Journal of Membrane Science 1976;1:17–32.
[19] Lee KH, Hwang ST. The transport of condensible vapors through a microporous Vycor glass membrane. Journal of Colloid and Interface Science 1986;110:544–55.
[20] Rao MB, Sircar S. Nanoporous carbon membranes for separation of gas mixtures by selective surface flow. Journal of Membrane Science 1993;85:253–64.
[21] Rao MB, Sircar S. Performance and pore characterization of nanoporous carbon membranes for gas separation. Journal of Membrane Science 1996;110:109–18.
[22] Raharjo RD, Freeman BD, Paul DR, Sanders ES. Pure and mixed gas CH_4 and *n*-C_4H_{10} permeability and diffusivity in poly[1-(trimethylsilyl)-1-propyne]. Polymer 2007;48:7329–44.
[23] Masuda T, Isobe E, Higashimura T. Polymerization of 1-(trimethylsilyl)-1-propyne by halides of niobium(V) and tantalum(V) and polymer properties. Macromolecules 1985;18:841–5.
[24] Dorkenoo KD, Pfromm PH. Accelerated physical aging of thin poly[1-(trimethylsilyl)-1-propyne] films. Macromolecules 2000;33:3747–51.
[25] Langsam M, Robeson LM. Substituted propyne polymers – part II. Effects of aging on the gas permeability properties of poly[1-(trimethylsilyl)-1-propyne] for gas-separation membranes. Polymer Engineering and Science 1989;29:44–54.
[26] Nagai K, Freeman BD, Hill AJ. Effect of physical aging of poly[1-(trimethylsilyl)-1-propyne] films synthesized with $TaCl_5$ and $NbCl_5$ on gas permeability, fractional free volume, and positron annihilation lifetime spectroscopy parameters. Journal of Polymer Science, Part B: Polymer Physics 2000;38:1222–39.
[27] Nagai K, Nakagawa T. Effects of aging on the gas permeability and solubility in poly[1-(trimethylsilyl)-1-propyne] membranes synthesized with various catalysts. Journal of Membrane Science 1995;105:261–72.
[28] Yampol'skii YP, Shishatskii SM, Shantorovich VP, Antipov EM, Kuzmain NN, Rykov SV, et al. Transport characteristics and other physicochemical properties of aged poly[1-(trimethylsilyl)-1-propyne]. Journal of Applied Polymer Science 1993;48:1935–44.
[29] Hill AJ, Pas SJ, Bastow TJ, Burgar MI, Nagai K, Toy LG, et al. Influence of methanol conditioning and physical aging on carbon spin-lattice relaxation times of poly[1-(trimethylsilyl)-1-propyne]. Journal of Membrane Science 2004;243:37–44.
[30] Jia J. Gas separation and pervaporation of chemically modified poly[1-(trimethylsilyl)-1-propyne] membranes. Ph.D. dissertation. Michigan State University; 1999.
[31] Jia J, Baker GL. Crosslinking of poly[1-(trimethylsilyl)-1-propyne] membranes using bis(aryl azides). Journal of Polymer Science, Part B: Polymer Physics 1998;36:959–68.
[32] Ruud CJ, Jia J, Baker GL. Synthesis and characterization of poly[(1-trimethylsilyl-1-propyne)-*co*-(1-(4-azidobutyldimethylsilyl)-1-propyne)] copolymers. Macromolecules 2000;33:8184–91.
[33] Kelman SD, Matteucci S, Bielawski CW, Freeman BD. Crosslinking poly[1-(trimethylsilyl)-1-propyne] and its effect on solvent resistance and transport properties. Polymer 2007;48:6881–92.
[34] Dean JA. Lange's handbook of chemistry. 15th ed. New York: McGraw-Hill; 1999.
[35] Khodzhaeva VL, Zaikin VG, Khotimskii VS. Thermal oxidation of poly[1-(trimethylsilyl)-1-propyne] studied by IR spectroscopy. Russian Chemical Bulletin (Translation of Izvestiya Akademii Nauk, Seriya Khimicheskaya) 2003;52:1333–9.
[36] Andrady AL, Merkel TC, Toy LG. Effect of particle size on gas permeability of filled superglassy polymers. Macromolecules 2004;37:4329–31.
[37] De Sitter K, Winberg P, D'Haen J, Dotremont C, Leysen R, Martens JA, et al. Silica filled poly[1-(trimethylsilyl)-1-propyne] nanocomposite membranes: Relation between the transport of gases and structural characteristics. Journal of Membrane Science 2006;278:83–91.
[38] Pinnau I, He Z. Pure- and mixed-gas permeation properties of polydimethylsiloxane for hydrocarbon/methane and hydrocarbon/hydrogen separation. Journal of Membrane Science 2004;244:227–33.
[39] Jordan SM, Koros WJ, Fleming GK. The effects of carbon dioxide exposure on pure and mixed gas permeation behavior: comparison of glassy polycarbonate and silicone rubber. Journal of Membrane Science 1987;30:191–212.
[40] Dixon-Garrett SV, Nagai K, Freeman BD. Sorption, diffusion, and permeation of ethylbenzene in poly[1-(trimethylsilyl)-1-propyne]. Journal of Polymer Science, Part B: Polymer Physics 2000;38:1078–89.
[41] Merkel TC, Bondar V, Nagai K, Freeman BD. Sorption and transport of hydrocarbon and perfluorocarbon gases in poly[1-(trimethylsilyl)-1-propyne]. Journal of Polymer Science, Part B: Polymer Physics 2000;38:273–96.
[42] Kelman SD, Matteucci S, Bielawski CW, Freeman BD. The effect of crosslinking and fumed silica addition on the pure gas sorption and transport properties of poly[1-(trimethylsilyl)-1-propyne], submitted for publication.
[43] Freeman B, Pinnau I. Separation of gases using solubility-selective polymers. Trends in Polymer Science (Cambridge, United Kingdom) 1997;5:167–73.
[44] Matteucci S, Yampolskii Y, Freeman BD, Pinnau I. In: Yampolskii Y, Freeman BD, Pinnau I, editors. Material science of membranes for gas and vapor separation. New York: John Wiley & Sons; 2006. p. 1–47.
[45] Raharjo RD, Freeman BD, Sanders ES. Pure and mixed gas CH_4 and *n*-C_4H_{10} sorption and dilation in poly(dimethylsiloxane). Journal of Membrane Science 2007;292:45–61.
[46] Smith JM, Van Ness HC, Abbot MM. Chemical engineering thermodynamics. 5th ed. New York: McGraw Hill; 1995.
[47] Lin H, Freeman BD. Gas and vapor solubility in cross-linked poly(ethylene glycol diacrylate). Macromolecules 2005;38:8394–407.
[48] Wijmans JG, Baker RW. The solution-diffusion model: a review. Journal of Membrane Science 1995;107:1–21.
[49] Bird RB, Stewart WE, Lightfoot EN. Transport phenomena. 2nd ed. New York: John Wiley & Sons; 2005.
[50] Prabhakar RS, Raharjo R, Toy LG, Lin H, Freeman BD. Self-consistent model of concentration and temperature dependence of permeability in rubbery polymers. Industrial and Engineering Chemistry Research 2005;44:1547–56.
[51] Pinteala M, Harabagiu V, Simionescu BC, Guegan P, Cheradame H. Ionically conducting networks derived from PEO containing aziridine groups. Polymer International 1999;48:1147–54.
[52] CAB-O-SIL TS-530 treated fumed silica: technical data. Cabot Corp.; 1991.
[53] Yasuda N, Yamamoto S, Wada Y, Yanagida S. Photocrosslinking reaction of vinyl-functional polyphenylsilsesquioxane sensitized with aromatic bis(azide) compounds. Journal of Polymer Science, Part A: Polymer Chemistry 2001;39:4196–205.
[54] Nagai K, Higuchi A, Nakagawa T. Gas permeability and stability of poly(1-trimethylsilyl-1-propyne-*co*-1-phenyl-1-propyne) membranes. Journal of Polymer Science, Part B: Polymer Physics 1995;33:289–98.
[55] Shimomura H, Nakanishi K, Odani H, Kurata M. Effects of physical aging on permeation of gases in a disubstituted polyacetylene. Reports on Progress in Polymer Physics in Japan 1987;30:233–6.
[56] Jordan SM, Fleming GK, Koros WJ. Permeability of carbon dioxide at elevated pressures in substituted polycarbonates. Journal of Polymer Science, Part B: Polymer Physics 1990;28:2305–27.
[57] Raharjo RD, Freeman BD, Sanders ES. Pure and mixed gas CH_4 and *n*-C_4H_{10} sorption and dilation in poly[1-(trimethylsilyl)-1-propyne]. Polymer 2007;48:6097–114.
[58] Masuda T, Iguchi Y, Tang BZ, Higashimura T. Diffusion and solution of gases in substituted polyacetylene membranes. Polymer 1988;29:2041–9.
[59] Raharjo RD. Mixed gas sorption and transport study in solubility selective polymers. Ph.D. dissertation. University of Texas at Austin; 2007.